Article

Immunity

Splenic Dendritic Cells Survey Red Blood Cells for Missing Self-CD47 to Trigger Adaptive Immune Responses

Graphical Abstract

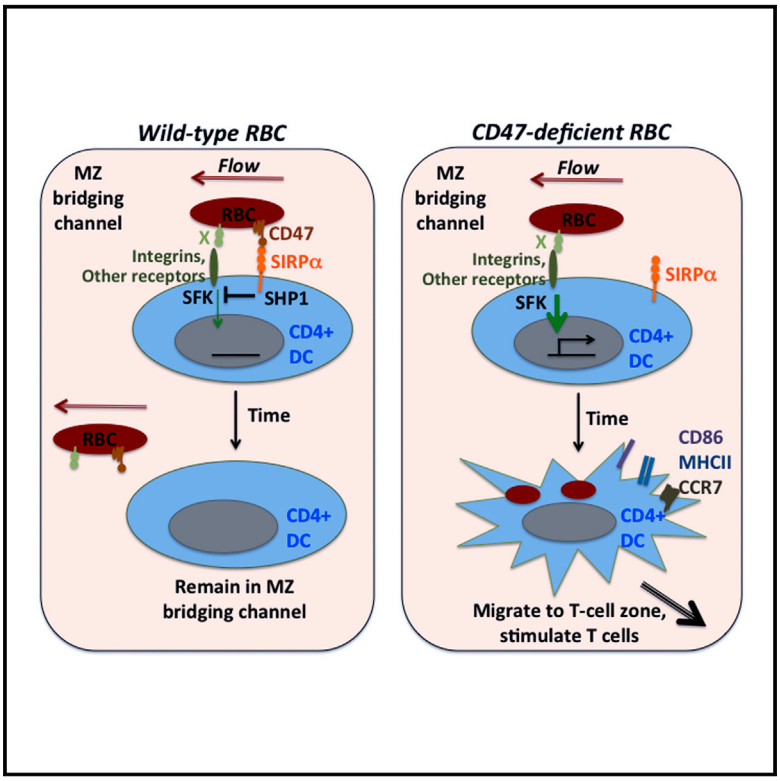

Authors

Tangsheng Yi, Jianhua Li, Hsin Chen, ..., Yongmei Hu, Clifford A. Lowell, Jason G. Cyster

Correspondence

jason.cyster@ucsf.edu

In Brief

SRBCs are a model antigen, but the mechanism for their adjuvant activity has been unclear. Cyster and colleagues demonstrate that sheep CD47 fails to engage mouse SIRPα and this causes SRBCs to activate splenic DCs. They suggest that DC activation by cells with reduced CD47 contributes to immunity against RBC-trophic pathogens.

Highlights

- SRBC adjuvant effect involves splenic DC activation by missing-self recognition
- CD47-deficient mouse RBCs have SRBC-like adjuvant activity
- Chronic DC activation in CD47-deficient mice might explain splenic DC deficiency
- RBC-triggered DC activation occurs via Src-family kinases and involves integrins

Accession Numbers

GSE71165

Yi et al., 2015, Immunity *43*, 764–775
October 20, 2015
http://dx.doi.org/10.1016/j.immuni.2015.08.021

CellPress

Immunity
Article

Splenic Dendritic Cells Survey Red Blood Cells for Missing Self-CD47 to Trigger Adaptive Immune Responses

Tangsheng Yi,[1,3] Jianhua Li,[1] Hsin Chen,[1] Jiaxi Wu,[1] Jinping An,[1] Ying Xu,[1] Yongmei Hu,[2] Clifford A. Lowell,[2] and Jason G. Cyster[1,*]

[1]Department of Microbiology and Immunology, University of California, San Francisco and Howard Hughes Medical Institute, CA 94143, USA
[2]Department of Laboratory Medicine, University of California, San Francisco, San Francisco, CA 94141, USA
[3]Present address: Department of Discovery Immunology, Genentech, South San Francisco, CA 94080, USA
*Correspondence: jason.cyster@ucsf.edu
http://dx.doi.org/10.1016/j.immuni.2015.08.021

SUMMARY

Sheep red blood cells (SRBCs) have long been used as a model antigen for eliciting systemic immune responses, yet the basis for their adjuvant activity has been unknown. Here, we show that SRBCs failed to engage the inhibitory mouse SIRPα receptor on splenic CD4$^+$ dendritic cells (DCs), and this failure led to DC activation. Removal of the SIRPα ligand, CD47, from self-RBCs was sufficient to convert them into an adjuvant for adaptive immune responses. DC capture of *Cd47*$^{-/-}$ RBCs and DC activation occurred within minutes in a Src-family-kinase- and CD18-integrin-dependent manner. These findings provide an explanation for the adjuvant mechanism of SRBCs and reveal that splenic DCs survey blood cells for missing self-CD47, a process that might contribute to detecting and mounting immune responses against pathogen-infected RBCs.

INTRODUCTION

The efficacy of xenogeneic red blood cells in promoting antibody responses is instrumental in elucidating key aspects of T cell help of immune responses (Hunter et al., 1974; Jerne and Nordin, 1963; Mitchell and Miller, 1968). In more recent years, SRBCs have been widely used as a simple method to elicit robust CD4$^+$ T cell and antibody responses and to elucidate requirements for germinal center (GC) and memory B cell generation (Dogan et al., 2009; Kraal et al., 1982; Shinall et al., 2000). Clinically, RBC immunogenicity is an important factor in the induction of alloantibody responses against minor histocompatibility antigens in 3%–6% of people receiving blood-group-matched RBC transfusions and a much higher frequency in people receiving Rhesus-antigen mismatched transfusions (Zimring and Hendrickson, 2008). RBC immunogenicity is also likely to be an important factor in the development of autoimmune hemolytic anemia. Given that RBCs lack or minimally express major histocompatibility complex (MHC) molecules and are infected by pathogens such as malaria that have had selective influences on the human population, it seems likely that specialized immune-sensing systems have evolved that contribute to RBC immunogenicity. However, despite the long period of study, the molecular basis for foreign RBC adjuvant activity has remained enigmatic.

The mouse spleen contains two major dendritic cell (DC) subsets, CD4$^+$ and CD8$^+$ DCs, with smaller numbers of double-negative DCs (Miller et al., 2012). CD4$^+$ DCs are best defined for their role in promoting CD4$^+$ T cell responses and, in turn, antibody responses, whereas CD8$^+$ DCs have a role in antigen cross-presentation to CD8$^+$ T cells (Miller et al., 2012). CD4$^+$ DCs, particularly those identified by co-expression of the lectin DCIR2, are enriched in regions of the spleen known as marginal zone (MZ) bridging channels, located between the T zone and red pulp (Witmer and Steinman, 1984). DC positioning in these channels is dependent on the chemoattractant receptor EBI2 (GPR183) (Gatto et al., 2013; Yi and Cyster, 2013). A specialized feature of the spleen is its open circulation; blood is released in the marginal sinus to then flow through the MZ and on to the red pulp (Mebius and Kraal, 2005). RBCs travel with this flow and, after passing through the macrophage-rich MZ and red pulp, return to circulation via venous sinuses (Mebius and Kraal, 2005). The positioning of CD4$^+$ DCs in the MZ bridging channel places them in a location that is exposed to RBCs (Yi and Cyster, 2013).

CD47 (also known as integrin-associated protein, IAP) is a cell surface protein expressed by most cell types, including RBCs (Barclay and Van den Berg, 2014; Oldenborg, 2013). CD47 engagement of the polymorphic signal regulatory protein α (SIRPα) on macrophages transmits a "don't eat me" signal that prevents cell engulfment. CD47-deficient RBCs, as well as various other cell types such as cancer stem cells, are rapidly cleared from circulation in wild-type (WT) mice but not in mice lacking SIRPα (Chao et al., 2012; Oldenborg, 2013). The SIRPα negative signal involves immunoreceptor tyrosine-based inhibitory motif (ITIM)-mediated recruitment of protein-tyrosine phosphatases (SHP1 and SHP2) that counteract pro-phagocytic signals (Barclay and Van den Berg, 2014; Oldenborg, 2013). The pro-phagocytic receptor-ligand systems that trigger phagocytosis of *Cd47*$^{-/-}$ cells are not well defined, but low-density lipoprotein (LDL)-related protein-1 (LRP1) on macrophages binding to calreticulin on target cells has been implicated in some situations (Chao et al., 2010; Gardai et al., 2005). Mice deficient in

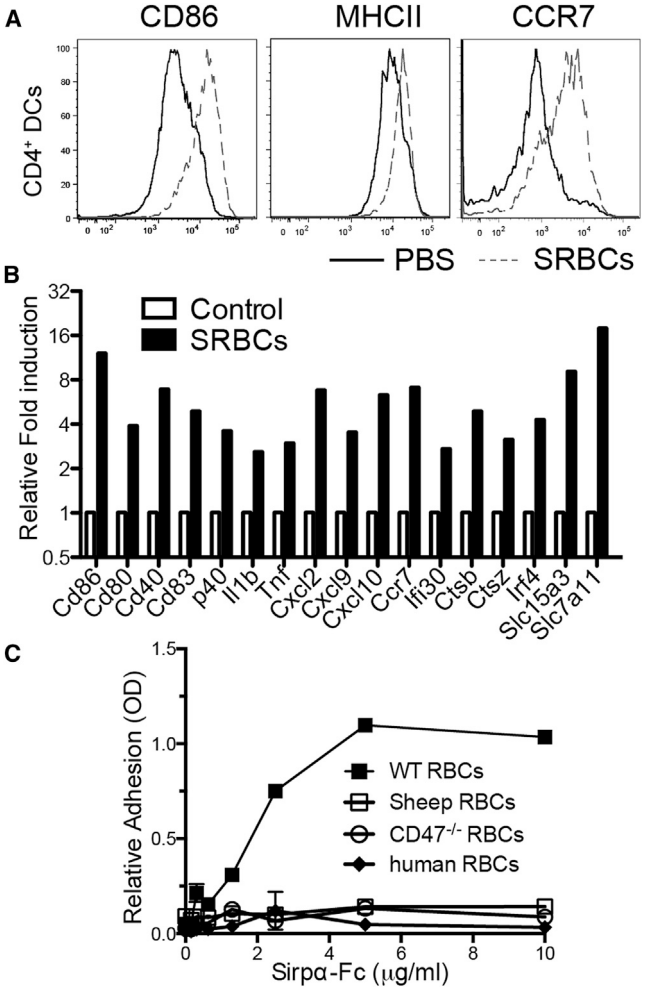

Figure 1. Xenogeneic RBCs Activate Splenic CD4⁺ DCs

(A) Mice were i.v. immunized with SRBC or PBS control and analyzed 3 hr later by flow cytometry for CD86, MHCII, and CCR7 in gated CD4⁺ DCs. One representative flow cytometry pattern is shown (n > 6 animals).

(B) Gene expression in CD4⁺ DCs from mice immunized with SRBCs 1 hr earlier relative to CD4⁺ DCs from PBS (control)-treated mice, determined by RNA-seq analysis. Average of two replicated experiments is shown. See also Table S1.

(C) Binding of WT or *Cd47*$^{-/-}$ mouse, sheep, and human RBCs to plate-bounded Sirpα-Fc. Points indicate mean ± SE (n = 3).The experiment was independently replicated three times with RBCs from different mice, sheep, and human donors. See also Figure S1.

CD47 or SIRPα have reduced numbers of CD4⁺ DCs, and this DC-deficiency has been associated with a reduced ability to mount antibody responses (Hagnerud et al., 2006; Saito et al., 2010; Van et al., 2006). However, the basis for the CD4⁺ DC deficiency in *Cd47*$^{-/-}$ or *Sirpa*$^{-/-}$ mice has not been elucidated.

CD47-SIRPα interactions are not well conserved across species, and we report here that sheep RBCs failed to bind mouse SIRPα. We show that SRBCs were strong activators of splenic CD4⁺ DCs, and we go on to show that removal of CD47 from mouse RBCs was sufficient to confer upon them "SRBC-like" immunogenicity. RBC-mediated splenic CD4⁺ DC activation occurred extremely rapidly (within minutes) and was then followed after 2–3 days by a DC depletion that phenocopied the splenic DC deficiency in *Cd47*$^{-/-}$ and *Sirpa*$^{-/-}$ mice. *Cd47*$^{-/-}$ RBC-mediated DC activation required signaling via Src-family kinases and was partially dependent on CD18-containing integrins. These data provide an explanation for the adjuvant activity of foreign RBCs and cells with reduced CD47 expression and they reveal a role for splenic MZ-bridging-channel DCs in self-RBC surveillance and in triggering immunity against RBCs.

RESULTS

SRBCs Activate Splenic CD4⁺ DCs and Promote Migration to the T Zone

During studies on EBI2-mediated MZ-bridging-channel positioning of CD4⁺ DCs, we observed that SRBCs could provoke DC CCR7 chemokine receptor upregulation and migration to the T cell zone (Yi and Cyster, 2013). Examining this process in detail, we found that within 6 hr of SRBC injection, splenic CD4⁺ DCs markedly upregulated CD86 and MHC class II (MHCII) as well as CCR7 (Figure 1A). This activation effect required intact SRBCs because it did not occur after injection of sonicated cells (Figure S1A). RNAseq analysis showed that 1 hr after SRBC injection, the DCs increased expression of transcripts for numerous maturation markers, including costimulatory molecules, lysosomal markers, and a range of cytokines and chemokines (Figure 1B and Table S1). Similar DC activation occurred after transfer of human RBCs (Figure S1B). Following injection, many foreign RBCs are captured in the splenic marginal zone by resident macrophages (Hagnerud et al., 2006; Yi and Cyster, 2013). However, ablation of these macrophages by treating *Cd169*-DTR mice with diphtheria toxin (DT) (Miyake et al., 2007) did not prevent DC activation by SRBCs (Figure S1C). Immunofluorescence microscopy of spleen tissue taken 15 min after PKH26-labeled SRBC injection revealed a close association between CD11c⁺ cells and PKH26 labeling in MZ bridging channels (Figure S1D). The DC activation occurred in mice lacking activating Fc receptor expression (*Fcer1g*$^{-/-}$) (Figure S1E) and in mice treated with cobra venom factor to deplete complement C3 (data not shown), ruling out an essential role for pre-existing (natural) xenoreactive immunoglobulin G (IgG) antibodies or the complement factor C3. We next considered whether CD47 might be involved. The CD47 receptor, SIRPα, is highly expressed on splenic CD4⁺ DCs (Lahoud et al., 2006; Figures S1F and S1G). SIRPα is polymorphic and known to often bind CD47 in a species-restricted manner (Barclay and Van den Berg, 2014; Oldenborg, 2013; Subramanian et al., 2006). In vitro adhesion assays showed that recombinant 129/Sv-derived mouse SIRPα supported adhesion of WT mouse RBCs, but it failed to support adhesion of sheep RBCs (Figure 1C) or, as expected (Subramanian et al., 2006), human RBCs (Figure 1C). Taken together, these data suggest that SRBCs might be causing CD4⁺ DC activation as a result of failing to adequately engage the negative regulatory SIRPα receptor on the DCs.

CD47-Deficient Self-RBCs Activate Splenic CD4⁺ DCs

We speculated that if a failure to engage the inhibitory SIRPα receptor was the basis for the SRBC adjuvant effect, then removing CD47 from mouse RBCs might be sufficient to make them stimulatory for CD4⁺ splenic DCs. Consistent with this

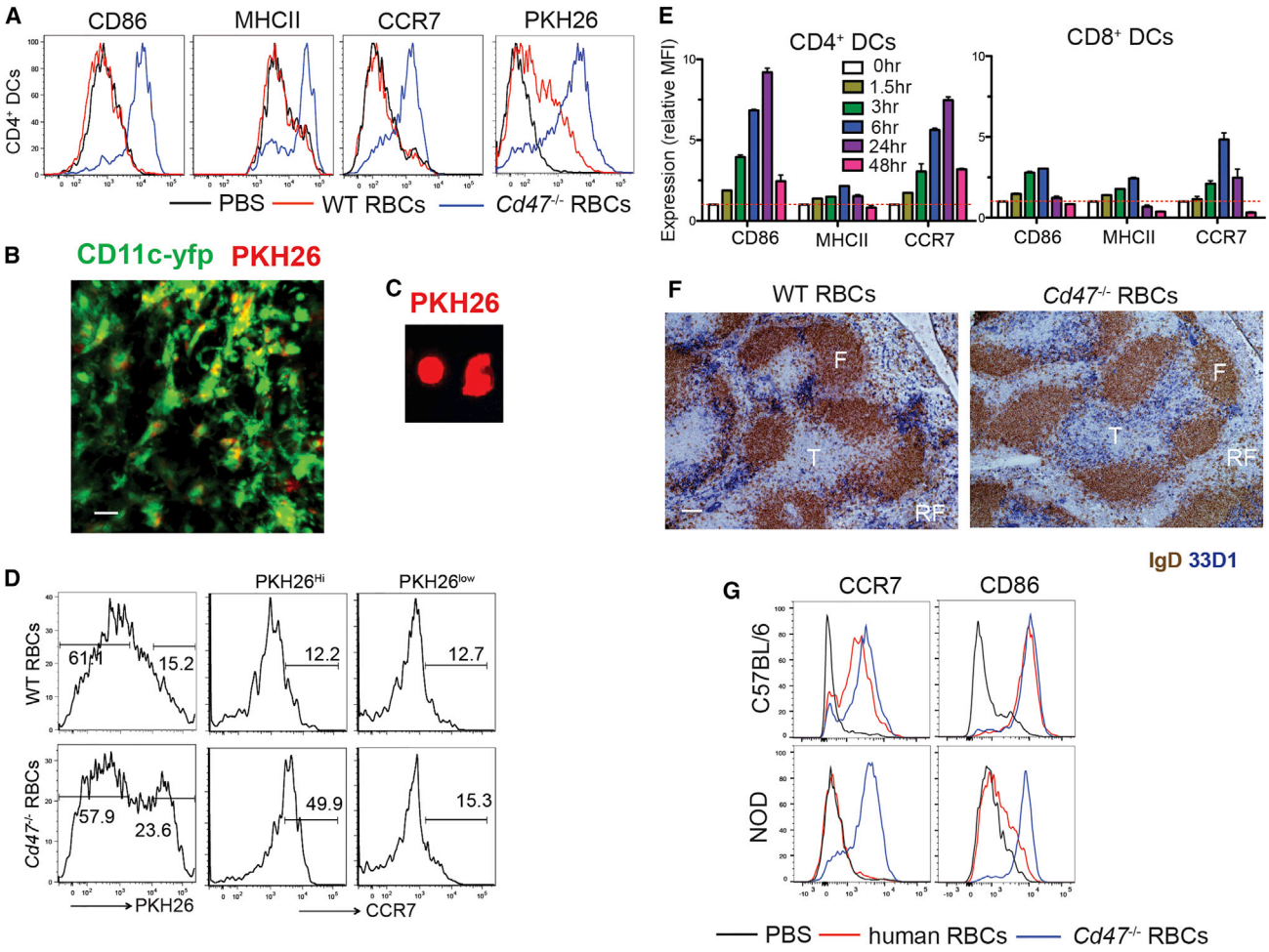

Figure 2. Activation and Uptake of CD47-Deficient RBCs by Splenic CD4$^+$ DCs

(A) Mice were immunized with 30 μl PKH26-labeled RBCs from WT or *Cd47*$^{-/-}$ mice and analyzed 3 hr later by flow cytometry for CD86, MHCII, CCR7, and PKH26 in gated CD4$^+$ DCs.

(B) CD11c-yfp mice were immunized with 30 μl PKH26-labeled RBCs from *Cd47*$^{-/-}$ mice. 20 min after immunization, spleens were vibratome sectioned and imaged with two-photon microscopy for YFP and PKH26. Scale bar, 20 μm. See also Movie S1.

(C) Fluoresce microscopy detection of PKH26 in flow cytometry sorted CD11c$^+$MHCII$^+$CD4$^+$ DCs from WT mice immunized 30 min earlier with PKH26-labeled *Cd47*$^{-/-}$ RBCs.

(D) Mice were i.v. immunized with 5 μl PKH26-labeled WT or *Cd47*$^{-/-}$ RBCs, and CD4$^+$ DCs were analyzed 3 hr later by flow cytometry for PKH26 and for CCR7. CCR7 staining is shown for CD4$^+$ DCs gated on PKH26^{hi} and PKH26^{lo} cells, as in plots on left.

(E) Mice were immunized with 30 μl *Cd47*$^{-/-}$ RBCs, and mean fluorescence intensity (MFI) of the indicated markers on gated CD4 or CD8$^+$ DCs relative to that of untreated mice was determined at the indicated time points (mean ± SE, n = 3).

(F) Mice were immunized with 30 μl WT or *Cd47*$^{-/-}$ RBCs, and 6 hr later, spleen sections were stained for DCIR2 (33D1, blue) and IgD (brown). F, follicle; T, T cell zone; RP, red pulp. Scale bar, 100 μm.

(G) C57BL/6 or NOD mice were i.v. immunized with PBS, human RBCs, and *Cd47*$^{-/-}$ RBCs, and analyzed 6 hr later by flow cytometry for CCR7 and CD86 in gated CD4$^+$ DCs. All above experiments have been independently replicated with at least 3–5 animals. See also Figure S2.

hypothesis, 3 hr after injection of *Cd47*$^{-/-}$ RBCs into WT mice, splenic CD4$^+$ DCs became uniformly CD86$^+$, MHCII^{hi}, and CCR7^{hi} (Figure 2A). Injection of *Cd47*$^{-/-}$ RBCs labeled with the red fluorescent membrane dye, PKH26, led to labeling of the majority of splenic CD4$^+$ DCs, indicating that they had captured RBC or RBC-derived molecules (Figure 2A). Two-photon microscopy of vibratome-cut spleens from *Itgax*-YFP$^+$ mice that had received PKH26-labeled *Cd47*$^{-/-}$ RBCs 20 min before revealed PKH26$^+$-material-bearing DCs that were situated in or near MZ bridging channels (Figure 2B and Movie S1). When splenic DCIR2$^+$ DCs were isolated by flow cytometry 30 min after PKH26-labeled *Cd47*$^{-/-}$ RBC injection and examined by microscopy, many of the DCs were positive for PKH26 labeling (Figure 2C).

As little as 5 μl of *Cd47*$^{-/-}$ blood was effective in promoting activation of splenic CD4$^+$ DCs (Figure S2A). When such low numbers of PKH26-labeled RBCs were injected, only a fraction of the CD4$^+$ DCs became dye labeled. Gating on the PKH26^{hi} versus PKH26^{lo} CD4$^+$ DCs showed that the activation occurred most completely in the cells that had directly captured labeled

RBCs or RBC fragments (Figure 2D), providing evidence that DC activation depended on physical contact with the *Cd47*$^{-/-}$ RBCs. The efficacy of *Cd47*$^{-/-}$ RBCs in causing DC activation was not influenced by the method of RBC preparation; blood isolated in Alsever's solution, EDTA, or heparin had similar DC-stimulating activity (Figure S2B). Injection of white blood cells isolated from 40 μl of *Cd47*$^{-/-}$ blood had no DC-stimulatory activity, confirming that the activation was RBC mediated (Figure S2C). Time course analysis showed surface CD86 and CCR7 upregulation occurring as early as 1.5 hr after *Cd47*$^{-/-}$ RBC injection and peaking after 6–24 hr (Figure 2E). CD8$^+$ DCs that express intermediate amounts of SIRPα and are sparse in the MZ showed much less activation and antigen capture (Figure 2E and Figures S1F, S1G, and S2D). Immunohistochemical staining of spleen sections showed that *Cd47*$^{-/-}$ RBCs caused CD4$^+$ DCs (identified by their co-expression of DCIR2) to rapidly relocate from the MZ bridging channels to the T cell zone, particularly the border region between the B and T cell zones (Figure 2F).

The above findings established that CD47 deficiency was sufficient to make mouse RBCs stimulatory for mouse DCs. We then asked the reciprocal question: is maintenance of the CD47-SIRPα interaction sufficient to prevent xenogeneic RBCs from causing DC activation? Previous work has shown that although human CD47 does not bind well to most strains of mouse SIRPα, it does bind strongly to the variant of SIRPα expressed in the non-obese diabetic (NOD) strain (Kwong et al., 2014; Takenaka et al., 2007). When human RBCs were transferred to NOD mice, DC activation did not occur, whereas it was readily observed when the mice received *Cd47*$^{-/-}$ mouse RBCs (Figure 2G). These findings further support the conclusion that lack of CD47-SIRPα engagement is the main mechanism for xenogeneic RBC-mediated activation of splenic DCs.

Splenic CD4$^+$ DC Deficiency in *Cd47*$^{-/-}$ Mice As a Result of Chronic Signaling

We speculated that if DC activation were occurring solely as a consequence of CD47-deficiency on RBCs, then short-term treatment with a SIRPα antagonistic antibody should similarly lead to CD4$^+$ DC activation. Consistent with this model, 6 hr after injection of a SIRPα function-blocking antibody (Oldenborg et al., 2000; Oldenborg et al., 2001; Wang et al., 2007), CD4$^+$ DCs, and to a much lesser extent CD8$^+$ DCs, showed upregulation of CD86, MHCII, and CCR7 (Figures 3A and S3A), and CD4$^+$ DCs relocated from MZ bridging channels into the T cell zone (Figure 3B). Previous work has shown that SIRPα- and CD47-deficient mice have a selective deficiency in splenic CD4$^+$ DCs (Hagnerud et al., 2006; Saito et al., 2010; Van et al., 2006; Figures S3B and S3C), but the basis for this deficiency has been unclear. We speculated that it might be a consequence of constant maturation-inducing signaling occurring in DCs as a result of the lack of an RBC CD47-triggered negative regulatory signal. Maturation-inducing signals of other types are known to shorten DC lifespan (De Trez et al., 2005). Flow cytometric analysis of the DCs remaining in *Cd47*$^{-/-}$ mice showed that the CD4$^+$ but not CD8$^+$ DCs had reduced SIRPα surface abundance, suggesting that the inhibitory receptor might be internalized in the absence of ongoing engagement with CD47 (Figure 3C). Importantly, when WT mice were injected with *Cd47*$^{-/-}$ RBCs, after the initial period of DC activation, the CD4$^+$ DCs became depleted, as assessed both by flow cytometry (Figure 3D, left panel) and immunohistochemistry for DCIR2 (Figure 2E). A similar CD4$^+$ DC depletion occurred 3 days after anti-SIRPα injection (Figure 3D, right panel). If CD4$^+$ DCs in *Cd47*$^{-/-}$ mice were continually being matured and depleted by endogenous RBCs, it seemed likely that they would be hypo-responsive to further stimulation by this pathway. A prior report found that *Cd47*$^{-/-}$ mice mounted poor antibody responses against SRBCs, though the defect was attributed to the reduction in DC number (Hagnerud et al., 2006). We found that the CD4$^+$ DCs remaining in *Cd47*$^{-/-}$ mice were not activated by SRBCs, whereas they were fully responsive to lipopolysaccharide (LPS) (Figure 3F).

Cd47$^{-/-}$ Self-RBCs Have Potent Adjuvant Activity

To test whether *Cd47*$^{-/-}$ mouse RBCs could function as an adjuvant for CD4$^+$ T cell responses, ovalbumin (OVA) was coupled to *Cd47*$^{-/-}$ or WT RBCs and injected into mice harboring OVA-specific OTII CD4$^+$ T cells. Marked proliferation of the OTII CD4$^+$ T cells occurred in the recipients of *Cd47*$^{-/-}$ but not in the recipients of WT OVA-RBCs (Figure 4A). A similar experiment with OVA-specific OTI CD8$^+$ T cells showed a lesser but still significant difference between mice receiving *Cd47*$^{-/-}$ and those receiving WT OVA-RBCs (Figure 4A). Phenotypic analysis of the responding CD4$^+$ OTII T cells at day 3 showed that they upregulated ICOS, PD1, and CXCR5, markers of follicular helper T cells (Figures 4B and S4D). When mice were immunized with OVA-coupled DCIR2 antibody, *Cd47*$^{-/-}$ RBCs again had an adjuvant effect, indicating that their action was through DC activation and not solely through promoting capture of RBC-bound antigen (Figure S4A). No OTII T cell proliferation was observed in mice treated with *Cd47*$^{-/-}$ RBCs in the absence of OVA (Figure S4B). In another approach, we tested whether the DC activation occurring after SIRPα blockade (Figure 2) was sufficient to augment T cell responses. In mice immunized with OVA-coupled DCIR2 antibody, SIRPα blockade led to increased proliferation of OVA-specific T cells (Figure S4C).

We speculated that if the adjuvant activity of SRBCs occurs by DCs binding these xenogeneic cells but failing to receive a SIRPα-negative signal, then this pathway should be disrupted in *Cd47*$^{-/-}$ hosts as a result of SIRPα already being fully disengaged and unable to distinguish SRBCs from endogenous RBCs. Consistent with this interpretation, OTII T cells showed 80% lower expansion in *Cd47*$^{-/-}$ hosts than in WT hosts in response to OVA-SRBCs (Figure 4C) and less induction of PD1 and ICOS (Figure S4D). In accordance with this defect, the *Cd47*$^{-/-}$ hosts failed to mount a GC response to SRBCs, as examined by flow cytometry (Figure 4D) and immunohistochemistry via the GL7 GC marker (Figure 4E). In comparison to *Cd47*$^{-/-}$ mice, *Ebi2*$^{-/-}$ mice have a similar deficiency in CD4$^+$ DC numbers (Gatto et al., 2013; Yi and Cyster, 2013), but they are expected to have intact SIRPα function, and they had normal DC SIRPα expression (Figure S4F); these mice mounted a GC response of normal magnitude after SRBC immunization (Figure 4F). Moreover, the *Cd47*$^{-/-}$ mice mounted a normal splenic GC response to viral-like particles (VLPs) that contain Toll-like receptor (TLR)-stimulating nucleic acids (Figure 4F). These

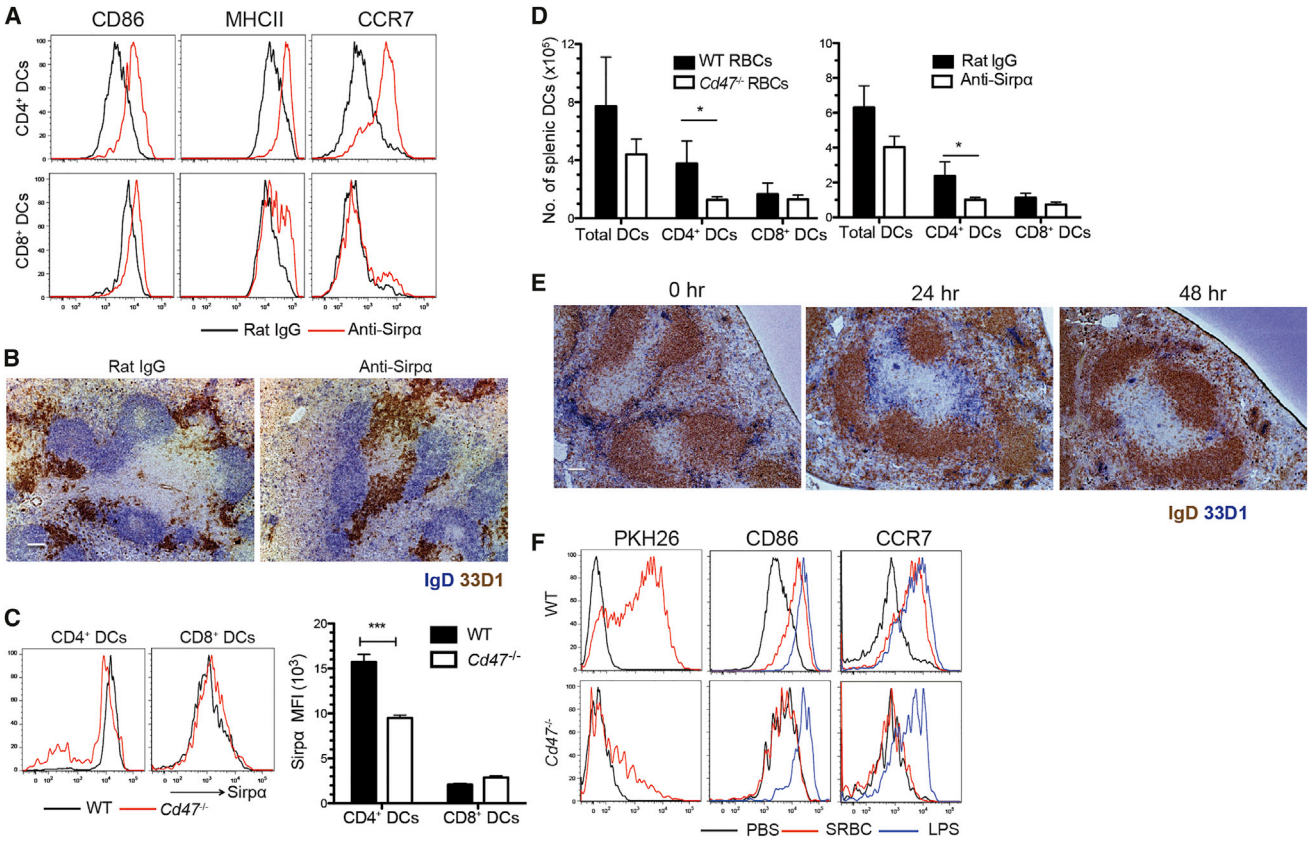

Figure 3. Blockade of Sirpα Activates Splenic CD4⁺ DCs and Leads to Their Loss

(A) Mice were i.v. injected with anti-Sirpα or control rat IgG2a and analyzed 6 hr later by flow cytometry for CD86, MHCII, and CCR7 in gated CD4 and CD8⁺ DCs (n = 3 mice).

(B) Immunochemistry staining of IgD and DCIR2 (33D1) in splenic sections from mice treated as in (A). Scale bar, 100 μm.

(C) Flow cytometric analysis of Sirpα expression in gated CD4⁺ and CD8⁺ DCs from WT or *Cd47*$^{-/-}$ mice. Left panel, representative flow cytomtery pattern; right panel, MFI of Sirpα expression (mean ± SE, n = 3 mice from two experiments).

(D) Mice were i.v. injected with 30 μl *Cd47*$^{-/-}$ RBCs or anti-Sirpα, and numbers of splenic DCs were quantified 3 days later by flow cytometry (mean ± SE, n = 3 mice).

(E) Mice were i.v. injected with *Cd47*$^{-/-}$ RBCs, and spleen sections were stained for IgD and DCIR2 (33D1) at the indicated time points. Scale bar, 100 μm.

(F) WT or *Cd47*$^{-/-}$ mice were i.v. injected with PBS, 30 μl PKH26-labeled SRBCs, or 20 μg LPS and then analyzed 3 hr later by flow cytometry for PKH26, CD86, and CCR7 in gated CD4⁺ and CD8⁺ DCs. One representative flow cytometry pattern is shown (n = 6 mice from two experiments). See also Figure S3.

observations support the conclusion that SRBCs activate the mouse immune system by failing to engage SIRPα on DCs.

Self-RBCs Activate CD4⁺ DCs via Src-Family Kinase Signaling

Cd47$^{-/-}$ mouse RBCs were effective in promoting CD4⁺ DC activation in mice lacking Myd88 and Trif, thus excluding a requirement for TLR receptors in RBC-triggered DC activation (Figure 5A). Given that SIRPα is generally thought to inhibit signaling by recruiting protein tyrosine phosphatases (particularly SHP1 in myeloid cells) (Oldenborg, 2013; Oldenborg et al., 2001), we tested whether Src-family tyrosine kinases (SFKs) were required for *Cd47*$^{-/-}$ RBC-mediated DC activation. Analysis of mice lacking individual SFKs Hck, Fgr, or Lyn, all known to be important in neutrophil and macrophage signaling (Abram and Lowell, 2009), showed little effect on the DC response (Figure S5A), but when Hck, Fgr, and Lyn were all removed, DC activation and repositioning in response to *Cd47*$^{-/-}$ RBCs was blocked (Figures 5B and 5C), whereas activation by LPS remained intact (Figure S5B). Hck, Fgr, and Lyn triple-deficient mice had normal or increased numbers of CD4⁺ DCs, and they were positioned comparably to WT cells (Figures 5C and S5C). Similar DC activation defects were observed in mixed bone marrow (BM) chimeras, establishing that the SFK requirement was DC intrinsic (Figure 5D and Figure S5D). As a further test of the DC SFK requirement, we generated 50:50 mixed SFK-deficient:*Zbtb46*-DTR BM chimeras and treated them with DT to ablate the WT DCs and leave only SFK-deficient DCs. *Cd47*$^{-/-}$ RBCs again failed to activate the SFK-deficient DCs (Figure S5E). Syk often functions downstream of SFKs (Lowell, 2011), and, consistent with this kinase contributing to DC activation, CCR7 was less completely induced in CD4⁺ DCs in *Syk*$^{-/-}$ fetal liver chimeras that had been injected with *Cd47*$^{-/-}$ RBCs or SRBCs (Figure S5F). Analysis of downstream signaling revealed rapid in vivo upregulation of phospho-p38, pS6, pERK, and pCREB in a SFK-dependent manner in CD4⁺ DCs after *Cd47*$^{-/-}$ RBC

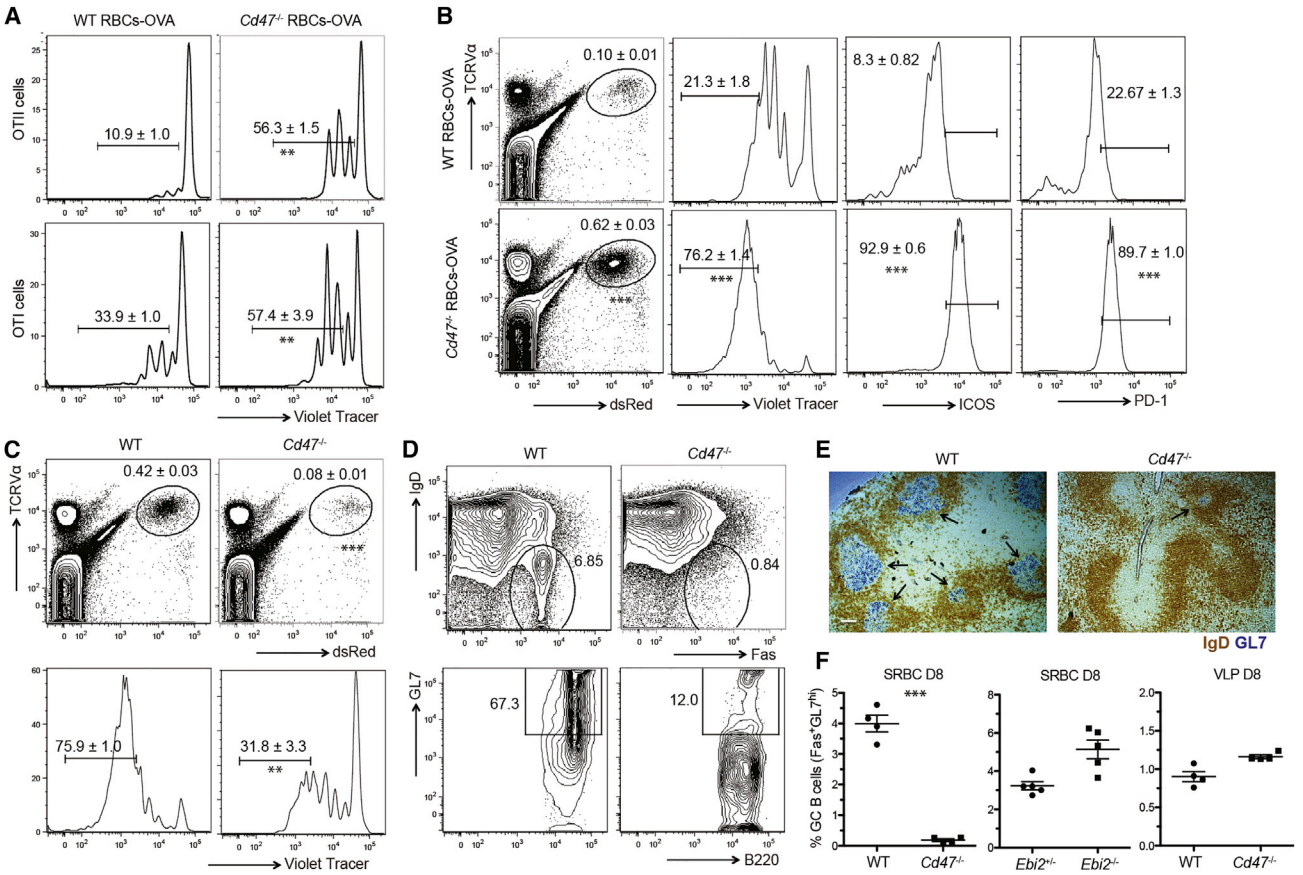

Figure 4. Adjuvant Effect of CD47-Deficient RBCs in CD4$^+$ T Cell Responses

(A and B) CD45.1$^+$ OTII or OTI splenocytes were labeled with cell trace violet, adoptively transferred to WT mice, and 1 day later mice were immunized with WT or *Cd47*$^{-/-}$ RBC-OVA conjugate. (A) Two days post-immunization, T cell proliferation was visualized by violet tracer dilution. (B) Three days post-immunization, frequency of OVA-specific OTII cells, violet tracer dilution, ICOS, and PD1 was examined by flow cytometry. Right three panels are gated on OTII T cells. Numbers on gates indicate mean (±SE) frequencies for three mice.

(C) CD45.1$^+$ OTII splenocytes were labeled with cell trace violet, adoptively transferred to WT or *Cd47*$^{-/-}$ mice, and 1 day later mice were immunized with SRBC-OVA conjugate. Frequency of OVA-specific OTII cells and violet tracer dilution on OTII cells was examined by flow cytometry 3 days post-immunization (mean ± SE, n = 3 mice).

(D– F) WT, *Cd47*$^{-/-}$ mice, *Ebi2*$^{+/-}$, and *Ebi2*$^{-/-}$ mice were immunized with SRBC or VLPs. Eight days after immunization, GC B cells were examined by flow cytometric analysis and immunochemistry staining. (D) Representative flow cytometric pattern. (E) Representative spleen sections; GCs are marked with black arrows. (F) Mean (±SE) frequency of IgD^{lo}Fas^{hi}GL7^{hi} GC B cells among total B cells in indicated mice. All experiments above were independently replicated at least two times with 3–5 mice each time. Scale bar in (E), 100 μm. **p < 0.01, ***p < 0.001 for unpaired Student's t test. See also Figure S4.

injection (Figures 5E and 5F). Phospho-p38 and pERK had already peaked 5 min after RBC injection, whereas pCREB reached a maximum at 60 min (Figure 5E).

CD18-Containing Integrins Are Involved in RBC-Mediated DC Activation

DC express a wide range of receptors capable of activating SFKs, though whether any of these molecules bind RBCs is not known (Sancho and Reis e Sousa, 2012). Many C-type lectin receptors depend on the ITAM-containing adaptors DAP12 or Fcεr1γ for surface expression and signaling (Lowell, 2011; Sancho and Reis e Sousa, 2012). Analysis of mice double-deficient for DAP12 (*Tyrobp*$^{-/-}$) and FcεRIγ showed that *Cd47*$^{-/-}$ RBCs induced DC activation normally (Figure 6A). Some receptors signal through another partner known as DAP10 (Lanier, 2009), but mice lacking the *Hcst* gene that encodes this co-receptor also activated normally in response to *Cd47*$^{-/-}$ RBCs (data not shown). Another important group of SFK-activating receptors are the integrins (Lowell, 2011). The CD18 (Itgβ2)-containing integrins CD11b and CD11c are defining markers of CD4$^+$ DCs (Steinman et al., 1997), and these cells also express high amounts of CD11a (LFA1) (Balkow et al., 2010). We found that *Cd47*$^{-/-}$ RBCs were inefficiently captured by DCIR2$^+$ CD4$^+$ DCs in *Itgb2*$^{-/-}$ mice, and the integrin-deficient DCs showed minimal activation (Figure 6B). The spleens of *Itgb2*$^{-/-}$ mice are enlarged due to myeloid hyperplasia in the red pulp (Scharffetter-Kochanek et al., 1998), making it possible that the requirement for CD18 was indirect. To test for an intrinsic integrin requirement, we established *Itgb2*$^{-/-}$:WT mixed BM chimeras. In these animals, the CD18-deficient cells were selectively compromised in capturing and becoming activated by *Cd47*$^{-/-}$ RBCs (Figures 6C and 6D). As a further method to test the intrinsic role of

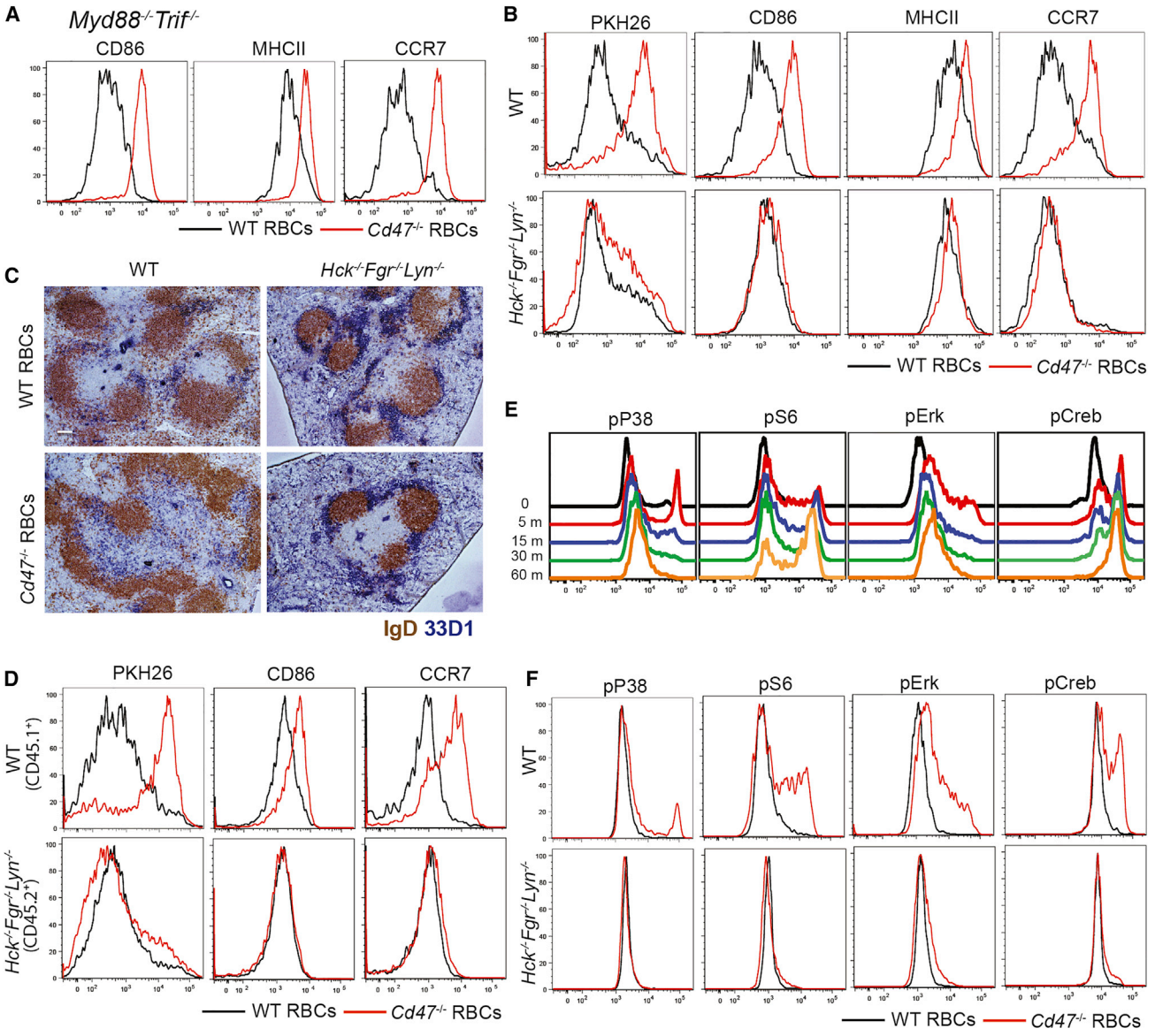

Figure 5. CD47-Deficient RBCs Activate Src-Family Kinase Signaling in CD4$^+$ DCs

(A) *Myd88*$^{-/-}$*Trif*$^{-/-}$ mice were immunized with WT or *Cd47*$^{-/-}$ RBCs and analyzed 3 hr later by flow cytometry for CD86, MHCII, and CCR7 in gated CD4$^+$ DCs (n = 2 mice).

(B and C) WT or *Hck*$^{-/-}$*Fgr*$^{-/-}$*Lyn*$^{-/-}$ mice were immunized with PKH26-labeled WT or *Cd47*$^{-/-}$ RBCs. (B) Flow cytometric analysis of PKH26, CD86, MHCII, and CCR7 in gated CD4$^+$ DCs 3 hr after immunization (n = 5 mice from 3 experiments). (C) Immunohistochemical staining of DCIR2 (33D1) and IgD in spleen sections taken 6 hr after immunization. Scale bar, 100 μm.

(D) WT CD45.1$^+$ mice were lethally irradiated and reconstituted with mixed BM cells (1:1 ratio) from CD45.1$^+$ WT mice and CD45.2$^+$ *Hck*$^{-/-}$*Fgr*$^{-/-}$*Lyn*$^{-/-}$ mice. Chimeras were immunized with PKH26-labeled WT or *Cd47*$^{-/-}$ RBCs and analyzed 3 hr later by flow cytometry for PKH26, CD86, and CCR7 in gated CD4$^+$ DCs (n = 4 mice in each group from two experiments).

(E) WT mice were immunized with *Cd47*$^{-/-}$ RBCs, and splenocytes were fixed at the indicated time points and phospho-p38, -S6, -Erk, and -Creb were examined in CD4$^+$ DCs by intracellular flow cytometric staining (n = 3 mice).

(F) WT or *Hck*$^{-/-}$*Fgr*$^{-/-}$*Lyn*$^{-/-}$ mice were immunized with WT or *Cd47*$^{-/-}$ RBCs for 5 min before staining, as in (E). One representative of three replicated experiments is shown. See also Figure S5.

CD18 in DCs, we generated mixed *Itgb2*$^{-/-}$:*Zbtb46*-DTR chimeras and treated the animals with DT to selectively ablate WT DCs prior to RBC injection. CD18-deficient DCs again showed reduced capture of *Cd47*$^{-/-}$ RBCs and less induction of CCR7 (Figure S6A). Tissue sections from these mice revealed that CD18-deficient and WT DCs were distributed similarly in control chimeras that received WT RBCs (Figure S6B), and there was incomplete relocalization of *Itgb2*$^{-/-}$ DCs to the outer T cell zone 6 hr after *Cd47*$^{-/-}$ RBC injection (Figure S6B). These findings provide evidence that CD18-containing integrins function

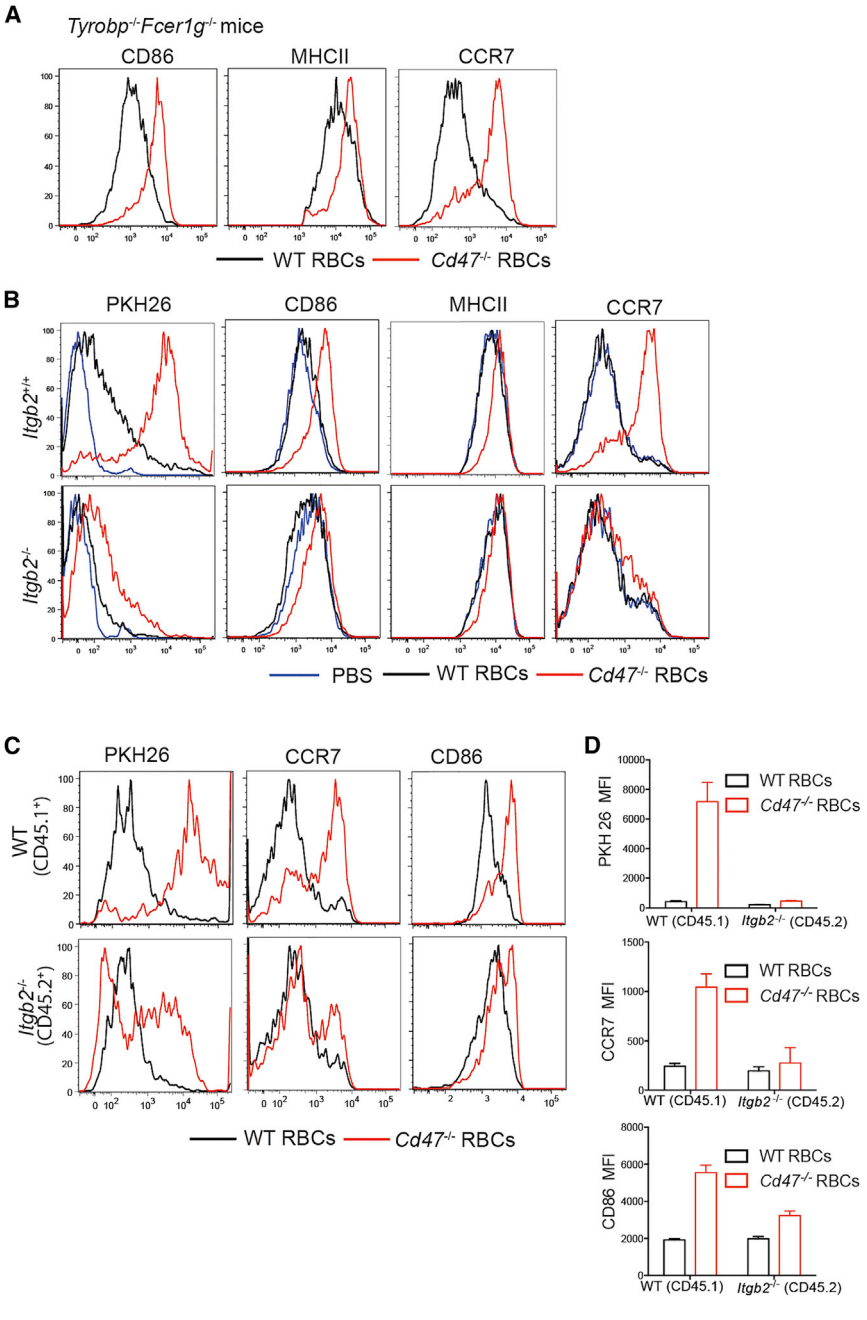

Figure 6. CD18-Integrin Involvement in RBC-Mediated DC Activation

(A) *Tyrobp*$^{-/-}$*Fcer1g*$^{-/-}$ mice were i.v. immunized with WT or *Cd47*$^{-/-}$ RBCs and analyzed 3 hr later by flow cytometry for CD86, MHCII, and CCR7 in gated CD4^{+} DCs (n = 4 mice from two experiments).

(B) *Itgb2*$^{+/+}$ and *Itgb2*$^{-/-}$ BM chimeras were immunized with PBS or PKH26-labeled WT or *Cd47*$^{-/-}$ RBCs. Flow cytometric analysis of PKH26, CD86, MHCII, and CCR7 in gated DCIR2 (33D1)$^{+}$ DCs 3 hr after immunization is shown (n = 5 mice in two experiments).

(C and D) WT CD45.1^{+} mice that had been reconstituted with a 1:1 mixture of BM cells from CD45.1^{+} WT and CD45.2^{+} *Itgb2*$^{-/-}$ mice were immunized with PKH26-labeled WT or *Cd47*$^{-/-}$ RBCs and analyzed 3 hr later. (C) Representative flow cytometry pattern for PKH26, CD86, and CCR7 in gated CD4^{+} DCs. (D) Mean (± SE) of MFI for the indicated markers (n = 3 mice). One representative of three replicated experiments is shown. See also Figure S6.

intrinsically in DCs during activation by CD47-deficient RBCs. However, some PKH26 acquisition and DC activation was still observable in each of these conditions, indicating that there are additional mechanisms of DC-RBC engagement and DC activation. Although LRP1 has been implicated in macrophage uptake of *Cd47*$^{-/-}$ apoptotic cells and RBCs by binding surface-exposed calreticulin (Gardai et al., 2005; Nilsson et al., 2012), *Lrp1*$^{-/-}$ DCs responded normally to *Cd47*$^{-/-}$ RBCs (Figure S6C). Finally, we tested the impact of CD18-integrin deficiency on the ability to mount CD4 T cell responses. When *Itgb2*$^{-/-}$ BM chimeras were immunized with OVA-conjugated *Cd47*$^{-/-}$ RBCs, they mounted a diminished WT OTII T cell proliferative response compared to the response in control BM chimeras (Figure S6D).

Taken together, these findings provide evidence that CD18-containing integrins contribute to the efficiency of DC activation by *Cd47*$^{-/-}$ self-RBCs.

DISCUSSION

CD47 is a marker of "self" on RBCs, and cells lacking CD47 are rapidly cleared from the bloodstream by macrophages (Oldenborg et al., 2000). Our findings provide evidence that splenic-bridging-channel DCs survey RBCs for missing self-CD47. When CD47 is absent or of a type unable to engage mouse SIRPα, CD4^{+} DCs are rapidly alerted and become competent to stimulate CD4 T cell and antibody responses. The concept of immune cell activation by missing-self recognition is best established for NK cell activation by cells with reduced or absent MHC class I (Lanier, 2005; Medzhitov and Janeway, 2002). NK cells utilize a family of ITIM-containing receptors that recognize self-MHC class I to inhibit signaling via activating receptors. Loss of CD47 from RBCs might act to alert DCs that RBCs are in an altered state in a similar way to how loss of MHC class I alerts NK cells that nucleated cells are in an altered state. MHC class I is downregulated during many types of viral infection and also on many cancer cells. We speculate that RBC CD47 becomes reduced or less accessible to SIRPα after infection by certain RBC-tropic pathogens, leading to DC activation and immunity.

The inhibitory "don't eat me" signal transmitted by SIRPα engagement in macrophages has been well characterized (Barclay and Van den Berg, 2014; Chao et al., 2012; Oldenborg, 2013), but the positive signal that it counteracts has been less

clear. We identify signaling via SFKs as an important positive signal in DCs. Our data support a model where, in the healthy state, RBC CD47 engagement of bridging-channel DC SIRPα transmits negative signals that override positive SFK signals from surface receptors, the RBC travels on to the red pulp, and the DC remains in a quiescent state. However, when CD47 surface amounts or availability are reduced, the positive SFK signals dominate over SIRPα negative signals, leading to RBC uptake and DC activation and movement to the T cell zone to promote cognate T cell and antibody responses. The uptake step, whether of intact RBC or RBC fragments, is likely to involve tyrosine phosphorylation of several cytoskeletal proteins, as observed during in vitro studies of IgG-opsonized SRBC phagocytosis by human macrophages (Tsai and Discher, 2008).

The factors influencing CD47 abundance on RBCs are not fully understood, but the amounts reduce gradually as the cells age (Oldenborg, 2013) and after periods of in vitro storage (Gilson et al., 2009; Stewart et al., 2005). CD47 in human RBCs exists in the membrane as a multiprotein complex (Oldenborg, 2013). Loss of some members of this complex, such as the Rh antigen or band 3, leads to reduced CD47 expression (Oldenborg, 2013). The membrane mobility and clustering of CD47 is also affected when components of the complex are missing (Oldenborg, 2013) and when membrane lipid composition changes (Lv et al., 2015). In mice, we found that *Cd47*$^{+/-}$ RBCs failed to stimulate DCs in WT recipients (data not shown), indicating that CD47 surface density might need to fall more than 50% to cause DC activation. However, CD47 in mouse RBCs is not in the same type of complex as human RBCs, making direct comparisons of mouse and human RBCs difficult (Oldenborg, 2013). In future studies, it might be possible to take advantage of our finding that NOD SIRPα adequately interacts with human CD47 to inhibit DC activation to test whether treatments, mutations, or infections that affect human CD47 abundance or distribution in the membrane diminish SIRPα engagement to an extent that leads to DC activation. Such studies might help discern whether this DC activation pathway contributes to the high frequency of autoimmune hemolytic anemia in Rh^{-} individuals (Oldenborg, 2013) and to the immunogenicity of stored allo-RBCs (Gilson et al., 2009; Hendrickson et al., 2010).

We suggest that positioning in MZ bridging channels allows CD4^{+} DCs to survey a large number of passing self-RBCs for altered or missing self-CD47 expression. White blood cells (WBCs) are also likely being surveyed in the same way, but given that RBCs outnumber WBCs by about 1,000 to 1, a major purpose of DC positioning in the bridging channels might be for exposure to the non-migratory RBCs. RBC engagement of DCs is likely to occur under fluid shear stress, providing forces that promote integrin-mediated adhesion and signaling (Woolf et al., 2007). Although RBCs express little if any of the CD18 integrin ligands ICAM1 or ICAM2, human and mouse RBCs express ICAM4 (Bailly et al., 1994; Bailly et al., 1995; Lee et al., 2006; Lee et al., 2003). In vitro studies have shown that human ICAM4 can bind all three CD18-containing integrins (Cartron and Elion, 2008; Ihanus et al., 2007; Lee et al., 2003). However, by using previously established *Icam4*$^{-/-}$ mice (Lee et al., 2006), we found that *Icam4*$^{-/-}$ *Cd47*$^{-/-}$ RBCs were captured by and activated DCs equivalently to *Icam4*$^{+/+}$ *Cd47*$^{-/-}$ cells (data not shown), suggesting that RBCs display additional ligands for CD18-containing integrins. Alternatively, it is possible that CD18-containing integrins are acting in an indirect way to augment DC access to RBCs. Although we did not observe major alterations in DC positioning in the spleens of DT-treated *Itgb2*$^{-/-}$ versus WT *Zbtb46*-DTR mixed BM chimeras, we cannot exclude the possibility that there are local cell-positioning or cell-cell interaction differences that affect the extent of exposure to rapidly moving blood cells. Additionally, given that we did detect measurable binding of *Cd47*$^{-/-}$ RBCs to *Itgb2*$^{-/-}$ DCs, there are likely to be further SFK-activating receptors on CD4^{+} DCs that have ligands on RBCs. Pro-phagocytic signaling during CD47-deficient cell binding by macrophages involves LRP1 engagement of surface-exposed calreticulin on target cells (Chao et al., 2010; Gardai et al., 2005). CD4^{+} DCs express only low amounts of LRP1 (Subramanian et al., 2014), and this receptor did not contribute to DC activation by RBCs. However, it remains plausible that other calreticulin receptors exist on DCs, and these could work together with integrins to promote DC activation.

Uptake of cancer cells by macrophages after CD47 blockade leads to antigen presentation and stimulation of CD8^{+} but not CD4^{+} T cell responses (Tseng et al., 2013). In that work, CD47-blocked target cells failed to activate DCs in vitro to a state with CD4^{+} T cell stimulatory properties (Tseng et al., 2013). Consistent with those observations, we were unable to observe activation of splenic DCs in vitro by SRBCs or *Cd47*$^{-/-}$ RBCs (data not shown). This could be a consequence of the background extent of DC maturation that occurs when splenic DCs are isolated and incubated in vitro, but it might also reflect a need for features of the in vivo environment, such as exposure to shear forces, that are not mimicked in the culture system. However, in vitro studies of human blood-derived DCs have revealed an ability of SIRPα engagement by CD47-Fc or RBCs to diminish DC activation (Latour et al., 2001; Schäkel et al., 2006). The basis for this discrepancy between mouse and human in vitro studies is unclear, but these data do suggest that our in vivo observations will translate to humans.

The basis for the CD4^{+} DC-deficiency in CD47- and SIRPα-deficient mice has been unclear (Hagnerud et al., 2006; Saito et al., 2010; Van et al., 2006), though one study provided evidence that engagement of DC SIRPα by CD47 on both hematopoietic and stromal cells is involved (Saito et al., 2010). By showing that blockade of SIRPα or transient treatment with *Cd47*$^{-/-}$ RBCs is sufficient to cause a similar deficiency of splenic CD4^{+} DCs after 3 days as full CD47- or SIRPα-deficiency, we provide support for a model in which unrestrained RBC-mediated transmission of activation signals causes sustained DC depletion. This model is consistent with the observation that SIRPα-deficient CD4^{+} DCs turn over at an accelerated rate (Saito et al., 2010). We speculate that RBC-triggered maturation of DCs is followed by their loss due to apoptosis as has been observed after splenic DC exposure to LPS (De Trez et al., 2005). We do not exclude the possibility that CD47 on additional cell types contributes to maintaining DC quiescence (Saito et al., 2010; Wang et al., 2007). CD47 and SIRPα-deficient mice have DC reductions in lymph nodes (LNs), the epidermis, and lamina propria, as well as in the spleen (Saito et al., 2010; Scott et al., 2014; Washio et al., 2015). Given that DCs in non-splenic locations might not be regularly exposed to RBCs, these deficiencies might indicate

that DC interactions with other CD47$^+$ cell types are important, but it is also possible that other functions of SIRPα and CD47 are needed in different DC types (Barclay and Van den Berg, 2014).

Finally, our demonstration that CD47-deficient RBCs can serve as adjuvants for CD4$^+$ T cell and antibody responses adds to recent literature highlighting CD47 antagonism as an approach to augment macrophage responses against cancer cells and parasite infected RBCs (Banerjee et al., 2015; Chao et al., 2012; Tseng et al., 2013). Induction of CD4$^+$ T cell and antibody responses during CD47-blockade treatments might contribute to anti-tumor and anti-pathogen effects. Such approaches could also be valuable in the design of vaccines for promoting immune responses against malaria and other RBC-tropic pathogens.

EXPERIMENTAL PROCEDURES

Mice

C57BL/6NCr and C57BL/6-cBrd/cBrd/Cr (CD45.1) mice at the ages of 7–9 weeks were purchased from the National Cancer Institute. NOD mice were from an internal University of California, San Francisco (UCSF) colony and were provided by Qizhi Tang. OVA-specific OTII or OTI TCR-transgenic mice and *Cd47*$^{-/-}$ and *Cd18*$^{-/-}$ mice were purchased from the Jackson Laboratory. *Ebi2*$^{-/-}$, *Lyn*$^{-/-}$, *Fgr*$^{-/-}$, *Hck*$^{-/-}$*Myd88*$^{-/-}$*Trif*$^{-/-}$, *Fcer1g*$^{-/-}$, *Fcer1g*$^{-/-}$*Tyrobp*$^{-/-}$, *Hcst*$^{-/-}$, *Lyn*$^{-/-}$*Fgr*$^{-/-}$*Hck*$^{-/-}$, and *Syk*$^{-/-}$ mice were previously established (Bakker et al., 2000; Lowell et al., 1994; Meng and Lowell, 1997; Pereira et al., 2009; Takai et al., 1994; Turner et al., 1995; Yamamoto et al., 2003) and have been backcrossed onto the C57BL/6 background for at least ten generations. CD169DTR mice (Miyake et al., 2007) were kindly provided by Masato Tanaka (RIKEN Research Center for Allergy and Immunology). Zbtb46-DTR mice (Meredith et al., 2012) were from the Jackson Laboratory. BM from *Lrp1*$^{flox/flox}$ CD11c$^{cre/+}$ mice (Subramanian et al., 2014) was provided by Ira Tabas (Columbia University). For BM or fetal liver chimeras, mice were lethally irradiated by exposure to 1,300 rads of γ-irradiation in two doses 3 hr apart, and BM cells or fetal liver cells (2×10^6 to 5×10^6) were transferred through the tail vein. Chimeric mice were in most cases analyzed 6–10 weeks after reconstitution. Diphtheria toxin (DT) (EMD Biosciences) was intraperitoneally injected in 1 μg doses at days −4 and −1 or as indicated, and the mice received RBCs at day 0. Animals were housed in a specific pathogen-free environment in the Laboratory Animal Research Center at UCSF, and all experiments conformed to ethical principles and guidelines approved by the Institutional Animal Care and Use Committee.

Virus-like Particles and LPS Immunization

Generation and packaging of virus-like particles (VLPs) containing bacteriophage Qβ antigens and CpG ODN G10 were described in detail previously (Jegerlehner et al., 2007). For mouse immunization and induction of GCs, mice were injected intraperitoneally with 50 μg VLPs-CpG. LPS (TLR grade) was obtained from Axxora, and mice were intravenously (i.v.) injected with 20 μg LPS.

Immunohistochemical Staining and Two-Photon Imaging

Cryosections of 7 μm were fixed and stained immunohistochemically as previously described (Allen et al., 2004) with the following antibodies: PE-conjugated anti-IgD (11-26c.2a, BioLegend), biotin-conjugated anti-GL7 (GL7, BioLegend), and FITC-conjugated 33D1 (33D1, BioLegend). Images were captured with a Zeiss AxioOberver Z1 inverted microscope. For multiphoton imaging, CD11cYFP mice were injected with PKH26-labeled (Sigma-Aldrich) *Cd47*$^{-/-}$ RBCs 20 min before the spleen was harvested and sectioned longitudinally with a vibratome (Leica). The cut spleen was perfused with RPMI1640 medium (Life Technologies) plus 10 mM HEPES and 95% CO_2 and 5% O_2. The cut spleen was imaged with a 7MP two-photon microscope (Carl Zeiss) equipped with a Chameleon laser (Coherent). Excitation wavelengths were 940 nm for YFP and 800 nm for PKH26. The z stack was 21 μm thick with 3 μm intervals. The image was acquired with ZEN2012 (Carl Zeiss), and the three dimensional movie was made with Imaris 7.4.2 ×64 (Bitplane).

CD47-Sirpα Adhesion Assay

A modified version of a previously reported assay was used (Subramanian et al., 2006). In brief, recombinant 129/Sv strain mouse Sirpα-Fc chimera protein (sequence ID P97797, R&D Systems) was coated on high-binding ELISA plates in serial dilutions. 129/Sv SIRPα is 96% identical to C57Bl/6 SIRPα, and the proteins have similar CD47 binding characteristics (Kwong et al., 2014; Takenaka et al., 2007). After overnight incubation at 4°C, plates were washed with PBS and blocked with Hanks Balanced Salt solution (HBSS) buffer containing 1% fatty-acid-free BSA at 37°C for 2 hr. After blockade, plates were washed twice, 50 μl RBCs (1×10^5/μl) diluted in HBSS with 1% BSA were added, and then the plates were incubated in a 37°C cell incubator for 1 hr. After incubation, non-adhered cells were washed away gently with PBS six times. Subsequently, 50 μl water was added to the wells for 30 min to completely lyse the adhered cells. RBCs have pseudoperoxidase activity of hemoglobin, and the relative numbers of RBCs were quantified by adding TMB peroxidase (HRP) substrate (Vector Laboratories) to RBC-water solution for 2–5 min. 25 μl stop solution (2M sulfuric acid) was then used to stop the reaction, and the plate was read at 450 nM with 540 nm as the correction wavelength. The dosage curve was calculated with a 4-parameter curve fit. An additional experiment was performed with a biotinylated fusion protein of C57BL/6 Sirpα domain 1 and rat CD4 domains 3 and 4 (Kwong et al., 2014), and this behaved similarly to the 129/Sv strain Sirpα-Fc in showing minimal binding of SRBC while supporting strong binding of WT mouse RBC.

RNA-Seq Analysis

Flow cytometric sorted DCs ($1.0 \times 10e^6$) were snap frozen in liquid nitrogen and stored at −80°C, and RNA was extracted with the QIAGEN RNeasy Kit. RNA quality was checked with the Agilent 2100 Bioanalyzer (RNA integrity number > 9 for all samples). Barcoded sequencing libraries were then generated with 100 ng of RNA with the Ovation RNA-Seq System V2 and Encore Rapid Library System. The UCSF Human Genetics Core performed next-generation sequencing (Illumina HiSeq 2500) with 100-bp paired-end reads. Sequences were reported as FASTQ files, which were aligned to the mm9 mouse genome with STAR (Spliced Transcript Alignment to a Reference). Generation of Log2FC values and further analyses were performed with a Bioconductor package on RStudio.

ACCESSION NUMBERS

RNA-seq data have been deposited in the Gene Expression Omnibus (NCBI) data repository under accession code GEO: GSE71165.

SUPPLEMENTAL INFORMATION

Supplemental Information includes Supplemental Experimental Procedures, six figures, one table, and one movie, and can be found with this article online at http://dx.doi.org/10.1016/j.immuni.2015.08.021.

ACKNOWLEDGMENTS

We thank Gregory Barton and Lewis Lanier for mice, Martin Bachmann for VLPs, Carl Gahmberg for 1A1 anti-ICAM4 antibody, Manikandan Subramanian, Ira Tabas, and Joachim Herz for *Lrp1*$^{fl/fl}$ *Itgax*-Cre$^+$ bone marrow, Neil Barclay, Lai Shan Kwong, and Chris Garcia for the B6 Sirpα reagents, and Robert Horton and Erick Lu for help with RNA-seq analysis and data deposition. T.Y. was a recipient of an Irvington postdoctoral fellowship from the Cancer Research Institute. J.G.C. is an investigator of the Howard Hughes Medical Institute. The work was supported in part by a grant from the NIH (AI40098).

Received: February 18, 2015
Revised: June 29, 2015
Accepted: August 25, 2015
Published: October 6, 2015

REFERENCES

Abram, C.L., and Lowell, C.A. (2009). The ins and outs of leukocyte integrin signaling. Annu. Rev. Immunol. *27*, 339–362.

Allen, C.D., Ansel, K.M., Low, C., Lesley, R., Tamamura, H., Fujii, N., and Cyster, J.G. (2004). Germinal center dark and light zone organization is mediated by CXCR4 and CXCR5. Nat. Immunol. *5*, 943–952.

Bailly, P., Hermand, P., Callebaut, I., Sonneborn, H.H., Khamlichi, S., Mornon, J.P., and Cartron, J.P. (1994). The LW blood group glycoprotein is homologous to intercellular adhesion molecules. Proc. Natl. Acad. Sci. USA *91*, 5306–5310.

Bailly, P., Tontti, E., Hermand, P., Cartron, J.P., and Gahmberg, C.G. (1995). The red cell LW blood group protein is an intercellular adhesion molecule which binds to CD11/CD18 leukocyte integrins. Eur. J. Immunol. *25*, 3316–3320.

Bakker, A.B., Hoek, R.M., Cerwenka, A., Blom, B., Lucian, L., McNeil, T., Murray, R., Phillips, L.H., Sedgwick, J.D., and Lanier, L.L. (2000). DAP12-deficient mice fail to develop autoimmunity due to impaired antigen priming. Immunity *13*, 345–353.

Balkow, S., Heinz, S., Schmidbauer, P., Kolanus, W., Holzmann, B., Grabbe, S., and Laschinger, M. (2010). LFA-1 activity state on dendritic cells regulates contact duration with T cells and promotes T-cell priming. Blood *116*, 1885–1894.

Banerjee, R., Khandelwal, S., Kozakai, Y., Sahu, B., and Kumar, S. (2015). CD47 regulates the phagocytic clearance and replication of the Plasmodium yoelii malaria parasite. Proc. Natl. Acad. Sci. USA *112*, 3062–3067.

Barclay, A.N., and Van den Berg, T.K. (2014). The interaction between signal regulatory protein alpha (SIRPα) and CD47: structure, function, and therapeutic target. Annu. Rev. Immunol. *32*, 25–50.

Cartron, J.P., and Elion, J. (2008). Erythroid adhesion molecules in sickle cell disease: effect of hydroxyurea. Transfus. Clin. Biol. *15*, 39–50.

Chao, M.P., Jaiswal, S., Weissman-Tsukamoto, R., Alizadeh, A.A., Gentles, A.J., Volkmer, J., Weiskopf, K., Willingham, S.B., Raveh, T., Park, C.Y., et al. (2010). Calreticulin is the dominant pro-phagocytic signal on multiple human cancers and is counterbalanced by CD47. Sci. Transl. Med. *2*, 63ra94.

Chao, M.P., Weissman, I.L., and Majeti, R. (2012). The CD47-SIRPα pathway in cancer immune evasion and potential therapeutic implications. Curr. Opin. Immunol. *24*, 225–232.

De Trez, C., Pajak, B., Brait, M., Glaichenhaus, N., Urbain, J., Moser, M., Lauvau, G., and Muraille, E. (2005). TLR4 and Toll-IL-1 receptor domain-containing adapter-inducing IFN-beta, but not MyD88, regulate Escherichia coli-induced dendritic cell maturation and apoptosis in vivo. J. Immunol. *175*, 839–846.

Dogan, I., Bertocci, B., Vilmont, V., Delbos, F., Mégret, J., Storck, S., Reynaud, C.A., and Weill, J.C. (2009). Multiple layers of B cell memory with different effector functions. Nat. Immunol. *10*, 1292–1299.

Gardai, S.J., McPhillips, K.A., Frasch, S.C., Janssen, W.J., Starefeldt, A., Murphy-Ullrich, J.E., Bratton, D.L., Oldenborg, P.A., Michalak, M., and Henson, P.M. (2005). Cell-surface calreticulin initiates clearance of viable or apoptotic cells through trans-activation of LRP on the phagocyte. Cell *123*, 321–334.

Gatto, D., Wood, K., Caminschi, I., Murphy-Durland, D., Schofield, P., Christ, D., Karupiah, G., and Brink, R. (2013). The chemotactic receptor EBI2 regulates the homeostasis, localization and immunological function of splenic dendritic cells. Nat. Immunol. *14*, 446–453.

Gilson, C.R., Kraus, T.S., Hod, E.A., Hendrickson, J.E., Spitalnik, S.L., Hillyer, C.D., Shaz, B.H., and Zimring, J.C. (2009). A novel mouse model of red blood cell storage and posttransfusion in vivo survival. Transfusion *49*, 1546–1553.

Hagnerud, S., Manna, P.P., Cella, M., Stenberg, A., Frazier, W.A., Colonna, M., and Oldenborg, P.A. (2006). Deficit of CD47 results in a defect of marginal zone dendritic cells, blunted immune response to particulate antigen and impairment of skin dendritic cell migration. J. Immunol. *176*, 5772–5778.

Hendrickson, J.E., Hod, E.A., Spitalnik, S.L., Hillyer, C.D., and Zimring, J.C. (2010). Storage of murine red blood cells enhances alloantibody responses to an erythroid-specific model antigen. Transfusion *50*, 642–648.

Hunter, P.M., Kappler, J.W., and Kettman, J.R. (1974). The frequency and activity of single helper T cells. J. Immunol. *113*, 830–834.

Ihanus, E., Uotila, L.M., Toivanen, A., Varis, M., and Gahmberg, C.G. (2007). Red-cell ICAM-4 is a ligand for the monocyte/macrophage integrin CD11c/CD18: characterization of the binding sites on ICAM-4. Blood *109*, 802–810.

Jegerlehner, A., Maurer, P., Bessa, J., Hinton, H.J., Kopf, M., and Bachmann, M.F. (2007). TLR9 signaling in B cells determines class switch recombination to IgG2a. J. Immunol. *178*, 2415–2420.

Jerne, N.K., and Nordin, A.A. (1963). Plaque Formation in Agar by Single Antibody-Producing Cells. Science *140*, 405.

Kraal, G., Weissman, I.L., and Butcher, E.C. (1982). Germinal centre B cells: antigen specificity and changes in heavy chain class expression. Nature *298*, 377–379.

Kwong, L.S., Brown, M.H., Barclay, A.N., and Hatherley, D. (2014). Signal-regulatory protein α from the NOD mouse binds human CD47 with an exceptionally high affinity– implications for engraftment of human cells. Immunology *143*, 61–67.

Lahoud, M.H., Proietto, A.I., Gartlan, K.H., Kitsoulis, S., Curtis, J., Wettenhall, J., Sofi, M., Daunt, C., O'keeffe, M., Caminschi, I., et al. (2006). Signal regulatory protein molecules are differentially expressed by CD8- dendritic cells. J. Immunol. *177*, 372–382.

Lanier, L.L. (2005). NK cell recognition. Annu. Rev. Immunol. *23*, 225–274.

Lanier, L.L. (2009). DAP10- and DAP12-associated receptors in innate immunity. Immunol. Rev. *227*, 150–160.

Latour, S., Tanaka, H., Demeure, C., Mateo, V., Rubio, M., Brown, E.J., Maliszewski, C., Lindberg, F.P., Oldenborg, A., Ullrich, A., et al. (2001). Bidirectional negative regulation of human T and dendritic cells by CD47 and its cognate receptor signal-regulator protein-alpha: down-regulation of IL-12 responsiveness and inhibition of dendritic cell activation. J. Immunol. *167*, 2547–2554.

Lee, G., Spring, F.A., Parsons, S.F., Mankelow, T.J., Peters, L.L., Koury, M.J., Mohandas, N., Anstee, D.J., and Chasis, J.A. (2003). Novel secreted isoform of adhesion molecule ICAM-4: potential regulator of membrane-associated ICAM-4 interactions. Blood *101*, 1790–1797.

Lee, G., Lo, A., Short, S.A., Mankelow, T.J., Spring, F., Parsons, S.F., Yazdanbakhsh, K., Mohandas, N., Anstee, D.J., and Chasis, J.A. (2006). Targeted gene deletion demonstrates that the cell adhesion molecule ICAM-4 is critical for erythroblastic island formation. Blood *108*, 2064–2071.

Lowell, C.A. (2011). Src-family and Syk kinases in activating and inhibitory pathways in innate immune cells: signaling cross talk. Cold Spring Harb. Perspect. Biol. *3*, a002352.

Lowell, C.A., Soriano, P., and Varmus, H.E. (1994). Functional overlap in the src gene family: inactivation of hck and fgr impairs natural immunity. Genes Dev. *8*, 387–398.

Lv, Z., Bian, Z., Shi, L., Niu, S., Ha, B., Tremblay, A., Li, L., Zhang, X., Paluszynski, J., Liu, M., et al. (2015). Loss of Cell Surface CD47 Clustering Formation and Binding Avidity to SIRPα Facilitate Apoptotic Cell Clearance by Macrophages. J. Immunol. *195*, 661–671.

Mebius, R.E., and Kraal, G. (2005). Structure and function of the spleen. Nat. Rev. Immunol. *5*, 606–616.

Medzhitov, R., and Janeway, C.A., Jr. (2002). Decoding the patterns of self and nonself by the innate immune system. Science *296*, 298–300.

Meng, F., and Lowell, C.A. (1997). Lipopolysaccharide (LPS)-induced macrophage activation and signal transduction in the absence of Src-family kinases Hck, Fgr, and Lyn. J. Exp. Med. *185*, 1661–1670.

Meredith, M.M., Liu, K., Darrasse-Jeze, G., Kamphorst, A.O., Schreiber, H.A., Guermonprez, P., Idoyaga, J., Cheong, C., Yao, K.H., Niec, R.E., and Nussenzweig, M.C. (2012). Expression of the zinc finger transcription factor zDC (Zbtb46, Btbd4) defines the classical dendritic cell lineage. J. Exp. Med. *209*, 1153–1165.

Miller, J.C., Brown, B.D., Shay, T., Gautier, E.L., Jojic, V., Cohain, A., Pandey, G., Leboeuf, M., Elpek, K.G., Helft, J., et al.; Immunological Genome Consortium (2012). Deciphering the transcriptional network of the dendritic cell lineage. Nat. Immunol. *13*, 888–899.

Mitchell, G.F., and Miller, J.F. (1968). Cell to cell interaction in the immune response. II. The source of hemolysin-forming cells in irradiated mice given bone marrow and thymus or thoracic duct lymphocytes. J. Exp. Med. *128*, 821–837.

Miyake, Y., Asano, K., Kaise, H., Uemura, M., Nakayama, M., and Tanaka, M. (2007). Critical role of macrophages in the marginal zone in the suppression of immune responses to apoptotic cell-associated antigens. J. Clin. Invest. *117*, 2268–2278.

Nilsson, A., Vesterlund, L., and Oldenborg, P.A. (2012). Macrophage expression of LRP1, a receptor for apoptotic cells and unopsonized erythrocytes, can be regulated by glucocorticoids. Biochem. Biophys. Res. Commun. *417*, 1304–1309.

Oldenborg, P.A. (2013). CD47: A Cell Surface Glycoprotein Which Regulates Multiple Functions of Hematopoietic Cells in Health and Disease. ISRN Hematol. *2013*, 614619.

Oldenborg, P.A., Zheleznyak, A., Fang, Y.F., Lagenaur, C.F., Gresham, H.D., and Lindberg, F.P. (2000). Role of CD47 as a marker of self on red blood cells. Science *288*, 2051–2054.

Oldenborg, P.A., Gresham, H.D., and Lindberg, F.P. (2001). CD47-signal regulatory protein alpha (SIRPalpha) regulates Fcgamma and complement receptor-mediated phagocytosis. J. Exp. Med. *193*, 855–862.

Pereira, J.P., Kelly, L.M., Xu, Y., and Cyster, J.G. (2009). EBI2 mediates B cell segregation between the outer and centre follicle. Nature *460*, 1122–1126.

Saito, Y., Iwamura, H., Kaneko, T., Ohnishi, H., Murata, Y., Okazawa, H., Kanazawa, Y., Sato-Hashimoto, M., Kobayashi, H., Oldenborg, P.A., et al. (2010). Regulation by SIRPα of dendritic cell homeostasis in lymphoid tissues. Blood *116*, 3517–3525.

Sancho, D., and Reis e Sousa, C. (2012). Signaling by myeloid C-type lectin receptors in immunity and homeostasis. Annu. Rev. Immunol. *30*, 491–529.

Schäkel, K., von Kietzell, M., Hänsel, A., Ebling, A., Schulze, L., Haase, M., Semmler, C., Sarfati, M., Barclay, A.N., Randolph, G.J., et al. (2006). Human 6-sulfo LacNAc-expressing dendritic cells are principal producers of early interleukin-12 and are controlled by erythrocytes. Immunity *24*, 767–777.

Scharffetter-Kochanek, K., Lu, H., Norman, K., van Nood, N., Munoz, F., Grabbe, S., McArthur, M., Lorenzo, I., Kaplan, S., Ley, K., et al. (1998). Spontaneous skin ulceration and defective T cell function in CD18 null mice. J. Exp. Med. *188*, 119–131.

Scott, C.L., Tfp, Z.M., Beckham, K.S., Douce, G., and Mowat, A.M. (2014). Signal regulatory protein alpha (SIRPα) regulates the homeostasis of CD103(+) CD11b(+) DCs in the intestinal lamina propria. Eur. J. Immunol. *44*, 3658–3668.

Shinall, S.M., Gonzalez-Fernandez, M., Noelle, R.J., and Waldschmidt, T.J. (2000). Identification of murine germinal center B cell subsets defined by the expression of surface isotypes and differentiation antigens. J. Immunol. *164*, 5729–5738.

Steinman, R.M., Pack, M., and Inaba, K. (1997). Dendritic cells in the T-cell areas of lymphoid organs. Immunol. Rev. *156*, 25–37.

Stewart, A., Urbaniak, S., Turner, M., and Bessos, H. (2005). The application of a new quantitative assay for the monitoring of integrin-associated protein CD47 on red blood cells during storage and comparison with the expression of CD47 and phosphatidylserine with flow cytometry. Transfusion *45*, 1496–1503.

Subramanian, S., Parthasarathy, R., Sen, S., Boder, E.T., and Discher, D.E. (2006). Species- and cell type-specific interactions between CD47 and human SIRPalpha. Blood *107*, 2548–2556.

Subramanian, M., Hayes, C.D., Thome, J.J., Thorp, E., Matsushima, G.K., Herz, J., Farber, D.L., Liu, K., Lakshmana, M., and Tabas, I. (2014). An AXL/LRP-1/RANBP9 complex mediates DC efferocytosis and antigen cross-presentation in vivo. J. Clin. Invest. *124*, 1296–1308.

Takai, T., Li, M., Sylvestre, D., Clynes, R., and Ravetch, J.V. (1994). FcR gamma chain deletion results in pleiotrophic effector cell defects. Cell *76*, 519–529.

Takenaka, K., Prasolava, T.K., Wang, J.C., Mortin-Toth, S.M., Khalouei, S., Gan, O.I., Dick, J.E., and Danska, J.S. (2007). Polymorphism in Sirpa modulates engraftment of human hematopoietic stem cells. Nat. Immunol. *8*, 1313–1323.

Tsai, R.K., and Discher, D.E. (2008). Inhibition of "self" engulfment through deactivation of myosin-II at the phagocytic synapse between human cells. J. Cell Biol. *180*, 989–1003.

Tseng, D., Volkmer, J.P., Willingham, S.B., Contreras-Trujillo, H., Fathman, J.W., Fernhoff, N.B., Seita, J., Inlay, M.A., Weiskopf, K., Miyanishi, M., and Weissman, I.L. (2013). Anti-CD47 antibody-mediated phagocytosis of cancer by macrophages primes an effective antitumor T-cell response. Proc. Natl. Acad. Sci. USA *110*, 11103–11108.

Turner, L., Ward, S.G., and Westwick, J. (1995). RANTES-activated human T lymphocytes. A role for phosphoinositide 3-kinase. J. Immunol. *155*, 2437–2444.

Van, V.Q., Lesage, S., Bouguermouh, S., Gautier, P., Rubio, M., Levesque, M., Nguyen, S., Galibert, L., and Sarfati, M. (2006). Expression of the self-marker CD47 on dendritic cells governs their trafficking to secondary lymphoid organs. EMBO J. *25*, 5560–5568.

Wang, H., Madariaga, M.L., Wang, S., Van Rooijen, N., Oldenborg, P.A., and Yang, Y.G. (2007). Lack of CD47 on nonhematopoietic cells induces split macrophage tolerance to CD47null cells. Proc. Natl. Acad. Sci. USA *104*, 13744–13749.

Washio, K., Kotani, T., Saito, Y., Respatika, D., Murata, Y., Kaneko, Y., Okazawa, H., Ohnishi, H., Fukunaga, A., Nishigori, C., and Matozaki, T. (2015). Dendritic cell SIRPα regulates homeostasis of dendritic cells in lymphoid organs. Genes Cells *20*, 451–463.

Witmer, M.D., and Steinman, R.M. (1984). The anatomy of peripheral lymphoid organs with emphasis on accessory cells: light-microscopic immunocytochemical studies of mouse spleen, lymph node, and Peyer's patch. Am. J. Anat. *170*, 465–481.

Woolf, E., Grigorova, I., Sagiv, A., Grabovsky, V., Feigelson, S.W., Shulman, Z., Hartmann, T., Sixt, M., Cyster, J.G., and Alon, R. (2007). Lymph node chemokines promote sustained T lymphocyte motility without triggering stable integrin adhesiveness in the absence of shear forces. Nat. Immunol. *8*, 1076–1085.

Yamamoto, M., Sato, S., Hemmi, H., Hoshino, K., Kaisho, T., Sanjo, H., Takeuchi, O., Sugiyama, M., Okabe, M., Takeda, K., and Akira, S. (2003). Role of adaptor TRIF in the MyD88-independent toll-like receptor signaling pathway. Science *301*, 640–643.

Yi, T., and Cyster, J.G. (2013). EBI2-mediated bridging channel positioning supports splenic dendritic cell homeostasis and particulate antigen capture. eLife *2*, e00757.

Zimring, J.C., and Hendrickson, J.E. (2008). The role of inflammation in alloimmunization to antigens on transfused red blood cells. Curr. Opin. Hematol. *15*, 631–635.